

Motion parameters estimation in dual-baseline Forward Scatter Radar configuration

N. Ustalli, D. Pastina, C. Bongioanni, P. Lombardo

*DIET Dept., Sapienza University of Rome
Via Eudossiana, 18- 00184 Rome, Italy*

{nertjana.ustalli, debora.pastina, carlo.bongioanni, pierfrancesco.lombardo}@uniroma1.it

Keywords: Forward scatter radar, motion parameters estimation, spectrogram, passive radar.

Abstract

The focus of this work is on the estimation of the motion parameters of moving targets by means of a dual receive antenna Forward Scatter Radar (FSR) configuration. For this purpose (i) the Doppler signature spectrogram for the single node FSR configuration and (ii) the time delay technique based on the cross-correlation between the signals acquired by a FSR system comprising two different receivers, are both analysed for the joint estimation of the baseline crossing point and of the cross baseline velocity. The proposed approach is assessed firstly through synthetic datasets by analysing different target trajectories. Finally, experimental results obtained by exploiting the FM signal as waveform of opportunity for the detection and motion estimation of air targets are shown to prove the applicability and the feasibility of the this approach.

1 Introduction

Forward Scatter Radar (FSR) systems are a subclass of Bistatic radar with a large bistatic angle close to 180° . The target radar cross-section (RCS) is typically enhanced in this region and is only slightly affected by absorbing coatings, [1]. The main restrictions of the FSR configuration are the loss of range resolution and the limited presence of the target shadow effect, that exists only within a narrow corridor around the baseline, [1].

In the past, different studies have shown the possibility to estimate the velocity using a single baseline FSR based on a matched filter ([1]) and spectrogram ([2]) approach assuming a priori knowledge in the other motion parameters. Moreover the possibility to estimate the kinematic parameters by means of a multi-node FSR system is shown in [3].

In this work we deal with the problem of motion parameters estimation taking advantage of a dual-baseline FSR configuration with one transmitter and two separated receivers. We exploit (i) the Doppler rate estimation through the spectrogram and (ii) the time delay estimation based on the cross-correlation between the signals acquired by the two receivers.

The proposed approach ensures the possibility to estimate two parameters namely the cross-baseline velocity and the baseline crossing point without requiring any a priori knowledge.

The performance of the proposed approach is firstly assessed against synthetic data for different target trajectories under the assumption that the target moves at constant velocity.

Finally, the feasibility and the effectiveness is demonstrated by applying it to recorded live data acquired with a dual-baseline FSR configuration exploiting FM signals as waveform of opportunity.

2 Forward scatter received signal model

In this work we consider a FSR configuration comprising one transmitter (Tx) and two different receivers (Rx_i for $i=1, 2$). The FSR geometry and the received signal model are briefly summarized in the following.

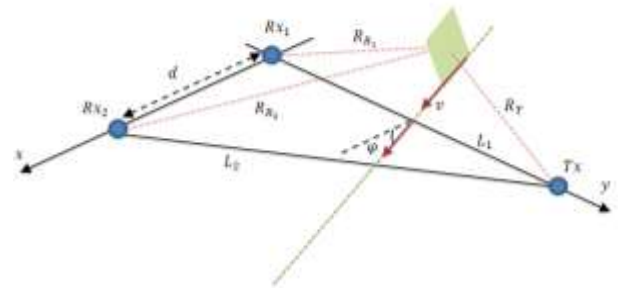


Fig. 1 - Dual-baseline FS radar geometry.

The coordinate system of the dual baseline configuration is shown in the in Fig. 1: the x and y axes specify the ground plane and the target follows a trajectory on the (x, y) plane. The first receiver, Rx_1 , is placed at the origin of the coordinate system (x, y) and the second receiver, Rx_2 is placed along the x -axis at a distance d from Rx_1 meanwhile the transmitter, Tx , is placed at $(0, L_1)$ along the y -axis.

The distances L_i ($i=1, 2$) between the transmitter and the receivers Rx_i , are indicated as baselines. It is assumed that the target follows a linear trajectory at a uniform speed v with direction specified by the angle φ with respect to x -axis. Therefore the target coordinates change with time, $\begin{cases} x(t) = x_0 + v_x t \\ y(t) = y_{01} + v_y t \end{cases}$; where is assumed $x_0 = 0$, y_{01} is the baseline crossing point of the first baseline, L_1 and (v_x, v_y) are the velocity components of v along the x and the y -axis, respectively. We assume that the target crosses the first baseline, L_1 at $t_c=0$ sec and the second baseline, L_2 at time $t_c=(L_1 - y_{01})d/(v_x L_1 + v_y d)$.

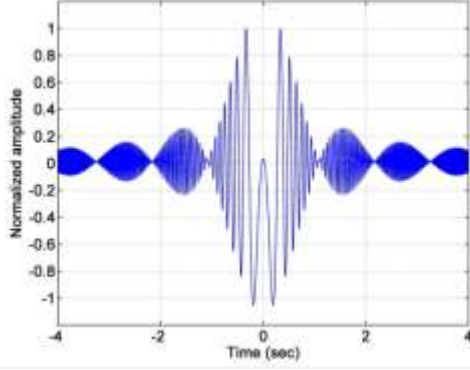


Fig. 2 Received signal after DC removal filter for a rectangular target crossing the baseline perpendicularly in the middle.

In accordance to this geometry, the range between transmitter and target and the range between the i -th receiver and target are defined respectively as follows:

$$\begin{cases} R_T(t) = \sqrt{x(t)^2 + [L_1 - y(t)]^2} \\ R_{R_i}(t) = \sqrt{x(t)^2 + [y(t) - (i-1)d]^2} \end{cases} \quad (1)$$

If possible interferences are disregarded at this stage, the signal at the input of the i -th receiver is the sum of the direct signal from transmitter to receiver and the scattered signal due to the presence of the target.

In this work it is assumed that a continuous waveform at an assigned carrier frequency is transmitted. In the literature, it is shown that the target scattered signal due to the target movement has an appropriate Doppler shift with an amplitude modulation specified by the FS pattern, which in turn depends on the shape of the shadow contour, on the motion parameters, and on the propagation losses, [1], [3]. In fact the target can be thought as a secondary antenna which has the silhouette of the target itself.

The Doppler signature carrying the kinematic information may be extracted following the processing scheme in [1]. The received signal, $r_i(t)$ for $i=1,2$ is passed through a square law detector, followed by a filtering stage to remove the continuous component (DC).

The resulting signal is a double-sided chirp signal, [1], and may be written as:

$$s_i(t) = \varepsilon_i(t) \sin \varphi_i(t) \quad (2)$$

where $\varepsilon_i(t)$ is the FS pattern and $\varphi_i(t)$ is the phase variation related to the i -th receiver.

In this work the 'shadow aperture' is approximated by a rectangular shape of horizontal dimension l_h and vertical dimension l_v , [3]. In (2) we assume that the phase shift of the target signal, with respect to the direct signal, is defined by the path difference:

$$\varphi_i(t) = \frac{2\pi}{\lambda} [R_T(t) + R_{R_i}(t) - L_i] \quad (3)$$

where λ is the wavelength.

By considering a Taylor expansion of the bistatic distance at the second order around the crossing time instant, in agreement with (1), equation (3) becomes:

$$\varphi_i(t) = \frac{\pi}{\lambda} v_x^2 \left(\frac{1}{L_i - y_{0i}} + \frac{1}{y_{0i}} \right) t^2 \quad (4)$$

which provides the double-sided chirp signal.

It is worth mentioning that the simplified model above applies when (i) the target dimensions are greater than the signal wavelength and the far field condition is satisfied for both the transmitter and the receivers (i.e. $R_T (R_{R_i})$ must be greater than $2\max(l_h, l_v)^2/\lambda$) and (ii) the angular separation between the two baselines is small.

Fig. 2 reports an example of the received signal after DC removal for a rectangular target that crosses the baseline perpendicularly in the middle: particularly the double-sided chirp phase is shown in noise free and far field conditions.

3 Motion parameters estimation approach

Taking advantage of the two baselines configuration previously introduced it is possible to estimate the cross baseline velocity, v_x and the baseline crossing point, y_0 without a priori knowledge of other kinematic parameters by means of a two-step approach as shown in the Fig. 3.

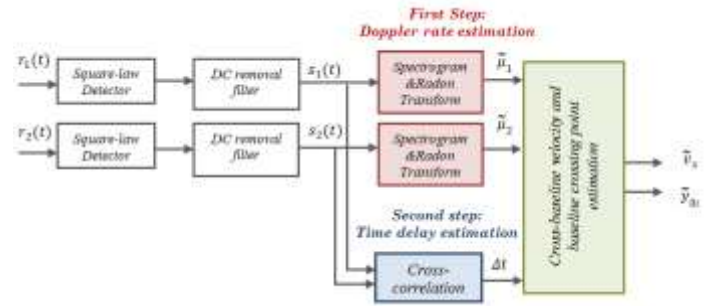


Fig. 3 Motion parameters estimation approach in dual baseline configuration.

Firstly, the signal at the output of the DC removal filter is analysed for the estimation of the Doppler rate through a time-frequency analysis such as the Short Time Fourier Transform (STFT). The STFT approaches the problem of determining when a particular frequency occurs by partitioning the signal into short segments and then applying a weighting function to the signal within each segment, prior to evaluating the Fourier transform, and is given by:

$$S_s(t, f) = \int_{-\infty}^{+\infty} w(\tau - t) s_i(\tau) e^{-j2\pi f \tau} d\tau \quad (5)$$

where $s_i(\tau)$ is defined in (2) and $w(\tau)$ is the analysis window centred at time t with duration T_w . The possibility to estimate the target velocity with the STFT for a target in FSR configuration, assuming a priori information on baseline crossing angle and baseline crossing point, has been shown in [2] and [4].

The spectrogram reported in the following is defined as the squared magnitude of the STFT, $|S_s(t, f)|^2$.

In agreement with (4), it is clear that the Doppler rate of the target signal is:

$$\mu_i = \frac{1}{2\pi} \frac{d\varphi_i(t)}{dt} = \frac{v_x^2}{\lambda} \left(\frac{1}{L_i - y_{0i}} + \frac{1}{y_{0i}} \right) \quad (6)$$

and is a function of the cross baseline velocity, v_x and of the baseline crossing point, y_{0i} , for an assigned system geometry (λ and L_i known). The Doppler rate, μ_i is extracted by applying

the Radon transform to the spectrogram, $|S_s(t, f)|^2$ as the absolute maximum observed in the Radon plane.

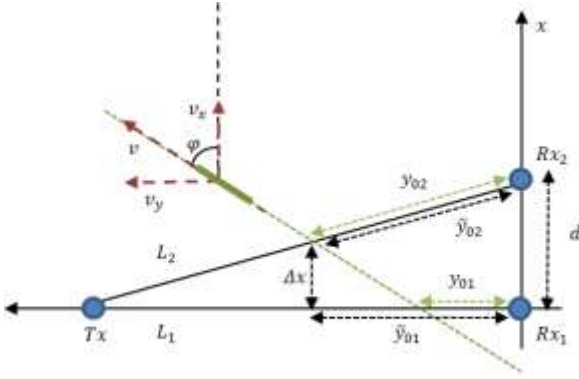


Fig. 4 –Top view of the dual-baseline configuration and baseline crossing point estimation.

Secondly, the time difference of arrival Δt , of the signals received at the two separated receivers is estimated through the cross-correlation.

Therefore, in accordance with the assumption of linear trajectory, the distance covered by the target between the two baselines in the elapsed time Δt , along the x -axis, is $\Delta x = v_x \Delta t$. In addition, drawing on this geometry (see Fig. 4) it is possible to estimate the baseline crossing point as function of the cross baseline velocity and the time delay in agreement with the following relation:

$$\Delta t = \frac{L_i - \tilde{y}_{0i}}{L_i} \frac{d}{v_x} \quad (7)$$

where \tilde{y}_{0i} is the estimated baseline crossing point. When the target crosses the baseline perpendicularly ($\varphi = 0^\circ$) the effective baseline crossing point is estimated. While for non-perpendicular baseline crossing angle, the estimated \tilde{y}_{0i} is not equal to the effective y_{0i} and the estimation error will depend on the baseline and on the baseline crossing angle.

Kinematic information extraction may be improved via multi-node FSR configuration, [3] nevertheless using only two receivers we observe that without a priori knowledge it is possible to unambiguously estimate two parameters, cross baseline velocity, v_x and baseline crossing point, y_{0i} .

In details, by exploiting the Doppler rate extraction from the spectrogram domain in (6) and the time delay, Δt estimation from the cross-correlation in (7), the estimated cross baseline velocity and baseline crossing point are:

$$\begin{cases} \tilde{v}_x = \frac{1}{\left(1 + \frac{1}{L_i \lambda \mu_i} \frac{d^2}{\Delta t^2}\right)} \frac{d}{\Delta t} \\ \tilde{y}_{0i} = \frac{1}{\left(\frac{1}{L_i} + \lambda \mu_i \frac{\Delta t^2}{d^2}\right)} \end{cases} \quad (8)$$

It is clear from (8) that for a long baseline the distance covered by the target between the two baselines can be assumed equal to the spacing between the two antennas, d and the cross baseline velocity may be approximated as $\tilde{v}_x \approx d/\Delta t$.

4 Performance analysis

In this section the performance of the proposed approach is assessed and discussed. For the analysis, four different target trajectories are investigated defined by the following baseline crossing point and baseline crossing angle: (A) $\varphi = 0^\circ$, $y_0 = L_1/2$, (B) $\varphi = 0^\circ$, $y_0 = L_1/4$, (C) $\varphi = 45^\circ$, $y_0 = L_1/2$ and (D) $\varphi = 45^\circ$, $y_0 = L_1/4$. For all the different case studies we consider a carrier frequency $f_c = 4.612 \text{ GHz}$ ($\lambda = 6.5 \text{ cm}$), a distance between the two receivers $d = 50 \text{ m}$, and baselines length equal to $L_1 = 6000 \text{ m}$, $L_2 = 6000.21 \text{ m}$. The results refer to a rectangular target larger than the wavelength with horizontal dimension $l_h = 2.5 \text{ m}$ and vertical dimension $l_v = 1.5 \text{ m}$ moving with a constant velocity $v = 36 \text{ m/s}$.

The results shown in the following are achieved for a noise free signal considering a long observation time corresponding to an observation angle $\Delta\theta = 10^\circ$. The observation angle is the angular interval from which the target is viewed: $\Delta\theta = 2tg^{-1}(v_x T_{obs}/L_i)$.

The dimension of the Hamming window for the estimation of the STFT in all case studies is set equal to $T_w = 0.3 \text{ s}$. Fig. 5 and Fig. 6 show the spectrograms (normalized with respect to its maximum value) of the signals received with both antennas related to the case (A) and (D).

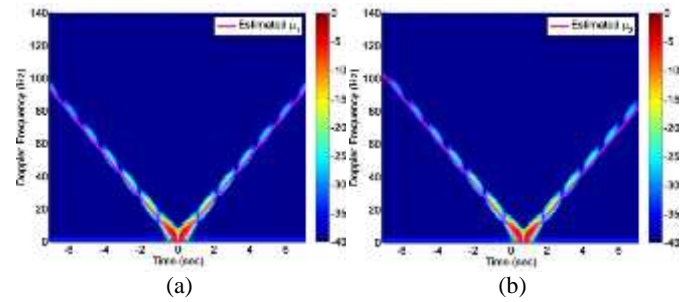


Fig. 5 - Spectrogram of the case (A) (a) of the signal received from Rx_1 and (b) of the signal received from Rx_2 .

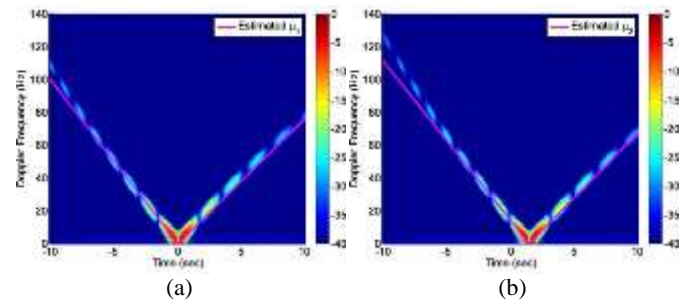


Fig. 6 - Spectrogram of the case (D) (a) of the signal received from Rx_1 and (b) of the signal received from Rx_2 .

It can be noted that a good estimation of the Doppler rate is provided which is obtained by applying the Radon transform to the spectrogram. The two red straight lines superimposed to the spectrogram represents the instantaneous Doppler frequency that vary linearly with time, $f_{d_i}(t) = \mu_i(t - t_c)$. The same good estimation of the Doppler rate is obtained for the case (B) and (C) even though here not reported for brevity. The cross-correlation of the signals at the output of the DC removal filter is then performed for the time delay estimation. Finally, in accordance with (8) the velocity cross-baseline and the baseline crossing point are estimated.

A good agreement with the corresponding effective values of \tilde{v}_x and \tilde{y}_{0i} is noted from the results reported in the Table I and Table II for all case studies. The cross baseline points of each baseline reported in the Table II are evaluated by considering the respective estimated Doppler rates, μ_i . This explains the greater error in the Case D for the second baseline as a larger error in the Doppler rate estimation is obtained with respect to the first baseline.

Table I Estimated velocity

	v_x (m/s)	\tilde{v}_x (m/s)	Error %
Case A	36	35.76	0.66
Case B	36	35.91	0.26
Case C	25.46	24.98	1.87
Case D	25.46	25.71	0.98

Table II Estimated baseline crossing point

	y_{01} (m)	\tilde{y}_{01} (m)	Error %	y_{02} (m)	\tilde{y}_{02} (m)	Error %
Case A	3000	3021.78	0.73	3000	3021.83	0.73
Case B	1500	1514.57	0.97	1500	1514.59	0.97
Case C	3000	3068.44	2.28	3024.79	3068.49	1.44
Case D	1500	1502.47	0.16	1537.19	1663.65	8.23

Some comments follow, related to the resolution capability in the spectrogram domain. First, if more than one target cross the single baseline at the same instant but with different Doppler rates the resolution capability of the spectrogram in the frequency domains depend on the observation time, T_{obs} and on the duration of the analysis window $w(t)$, T_w . Let μ' (i.e. $f_{d'}(t) = \mu'(t - t_c)$) and μ'' (i.e. $f_{d''}(t) = \mu''(t - t_c)$) be the Doppler rates of two targets crossing the single baseline at the same instant, t_c . So we have that the two targets can be separated in the spectrogram if:

$$(\mu' - \mu'') \frac{T_{obs}}{2} \geq \frac{\alpha}{T_w} \quad (9)$$

This mean that the Doppler rate difference should be:

$$\delta\mu \geq \frac{2\alpha}{T_{obs}T_w} \quad (10)$$

where values of α greater than 1 can be used for conservative specifications. It is clear that as the window analysis becomes shorter, the frequency resolution decreases. Also with the increasing of the observation time a better resolution is obtained.

If two targets with the same Doppler rate cross the baseline at different instants (i.e. $f_{d'}(t) = \mu(t - t_{c'})$ and $f_{d''}(t) = \mu(t - t_{c''})$ are the instantaneous Doppler frequencies of the first and the second target respectively) the targets can be separated in the spectrogram if:

$$\mu(t_{c'} - t_{c''}) \geq \frac{\alpha}{T_w} \quad (11)$$

where as previously values of α greater than 1 can be used for conservative specifications. This mean that the two targets can be separated if the time difference between the crossing instants is:

$$\delta t \geq \frac{\alpha}{\mu T_w} \quad (12)$$

where μT_w represents the Doppler bandwidth of the target in the time interval, T_w .

Finally, we can state that the length of the analysis window has to be chosen short enough since a linear phase term is compensated with the STFT but not so short as to sacrifice adequate resolution when two (or more) moving targets create Doppler-shifted return signals that are superimposed at the receiver.

We analyse now the same reference scenario with a baseline length equal to $L_1=6$ km and a carrier frequency equal to $f_c = 4.612$ GHz. Fig. 7 (a) shows the received signal after DC removal in the absence of noise where two targets with the same horizontal and vertical dimension (i.e. $l_h=2.5$ m and $l_v=1.5$ m) cross the baseline at the same instant, $t_c=0$ sec, in the middle with the same velocity of $v=36$ m/s but different angles. The first target crosses the baseline perpendicularly (i.e. $\varphi = 0^\circ$ and $\mu' = 13.29$ Hz/s) meanwhile the second target crosses the baseline with $\varphi = 20^\circ$ (i.e. $\mu' = 11.73$ Hz/s). An observation angle equal to $\Delta\theta = 10^\circ$ is considered that corresponds to an observation time equal to $T_{obs}=14.18$ s.

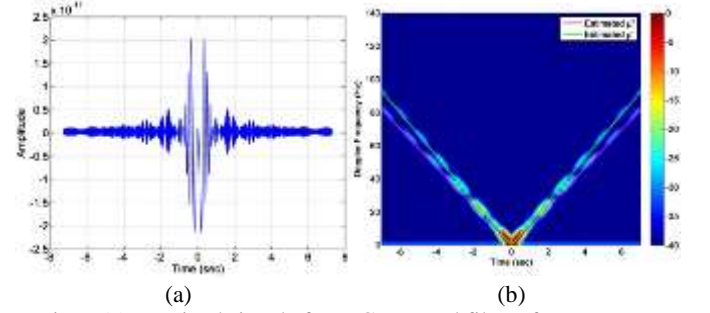


Fig. 7 (a) Received signal after DC removal filter of two targets crossing the baseline at the same instant with different Doppler rates and (b) the spectrogram.

Fig. 7 (b) shows the corresponding spectrogram obtained through a hamming window equal to $T_w=0.5$ s. It is noted that in the spectrogram domain the two targets with $\delta\mu = 1.55$ Hz/s are well separated. Now, for the same reference scenario and the same targets dimensions, the case of two targets following the same trajectory (same Doppler rate) but crossing the baseline at different instants is analysed.

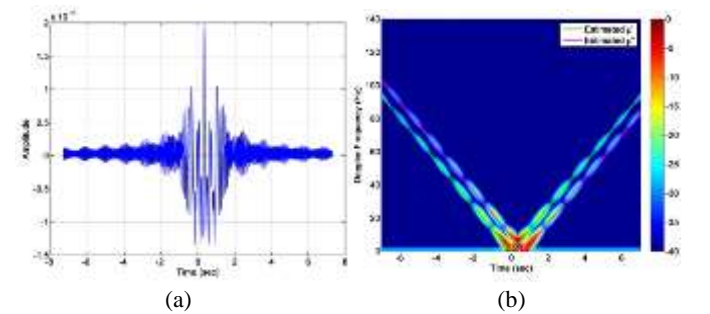


Fig. 8 (a) Received signal after DC removal filter of two targets crossing the baseline at different instants with the same Doppler rate and (b) the spectrogram.

Fig. 8(a) shows the received signal after DC removal for the case of two targets that cross the baseline perpendicularly in the middle with the same velocity of $v=36$ m/s but at different instants with a time difference between the crossing instants

equal to $\delta t = 0.7$ seconds. Fig. 8(b) shows the corresponding spectrograms: it is noted that the two targets are well resolved.

5 Application to real data

To test the effectiveness of the proposed approach a dual-baseline FSR configuration was set-up, exploiting FM signals as waveform of opportunity.

5.1 Acquisition campaign set-up

The experiment took place near the “Leonardo Da Vinci” airport (Rome, Italy) with the aim to detect planes landing at the 16L runway. Such non cooperative targets have been monitored through a commercial ADS-B receiver which provides useful information to be used as ground-truth for the velocity estimation. The two directive FM antennas, at a distance $d=9.1$ m from each other, are located at the sea side, 56 km (baseline) far from the selected transmitter located at Monte Gennaro. The antennas height is around 5 m, so a full visibility of the runway followed by the airplanes was achieved as near the airport tall buildings are not allowed. Moreover it is possible to retrieve φ and y_0 since the trajectory of the target during the approach to the 16L runway is known (i.e. provided by the local standard arrival procedure) and are equal to $\varphi=10^\circ$ and $y_0=5.19$ km, respectively. Also, as the distance d between the two antennas is small with respect to the baseline, the same y_0 is retrieved for both antennas. The multi-channel receiver is based on a direct Radio Frequency (RF) sampling approach. For each receiving channel, proper band-pass filters, variable attenuators and amplifiers are used in the analogue section to reject out-of-band interferences and to match the A/D dynamic range. After digital down-conversion of the acquired signals, single FM channels of interest are extracted, in particular in our case FM channel 107.4 MHz ($\lambda=2.85$ m) is considered.

5.2 Experimental results

Fig. 9 reports the signal received at both antennas related to a Boeing 737-800 with a horizontal and vertical dimension equal to 33.40 m and 11.13 m, respectively: the amplitude modulation due to the target movement is clearly visible.

It is worth mentioning that the gain of the two receiving chains is different, based on the disturbance received from each antenna. For this reason there is a difference in the signal level between $s_1(t)$ and $s_2(t)$, see Fig. 9. The signal at the output of the DC removal filter is analysed through STFT using a Hamming window with dimension equal to $T_w=2.56$ sec for the estimation of the Doppler rate, μ .

Fig. 10 and Fig. 11 show the spectrogram of the signal received from the first antenna, R_{x1} , and the second antenna, R_{x2} , respectively, normalized with respect to its maximum value. The target does not cross the baseline in the middle and perpendicularly so the two branches of the spectrograms are not completely symmetrical and two different Doppler rates are extracted from the Radon transform (see Fig. 12 and Fig. 13): $\tilde{\mu} = -0.4132$ and $\tilde{\mu} = 0.4533$. The same Doppler rate values are obtained from both antennas, R_{x1} and R_{x2} .

Then the cross-correlation is performed between the signals received at the two Rx antennas. To improve the cross-

correlation quality a part of the received signal is selected where the target signature is present (see Fig. 14).

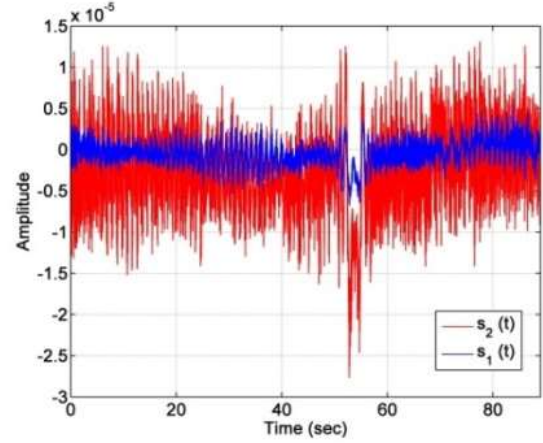


Fig. 9 - Received signal signature after DC removal filter from both antennas.

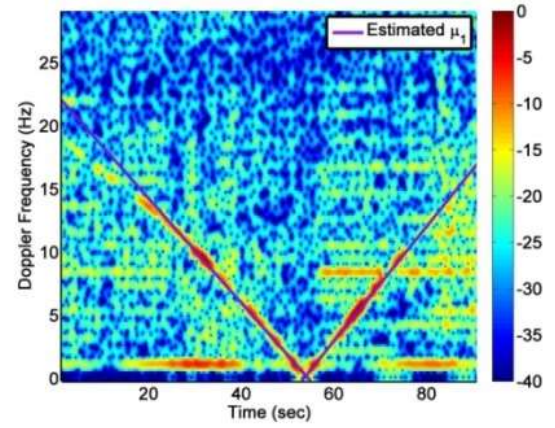


Fig. 10 - Spectrogram of the signal received from R_{x1} .

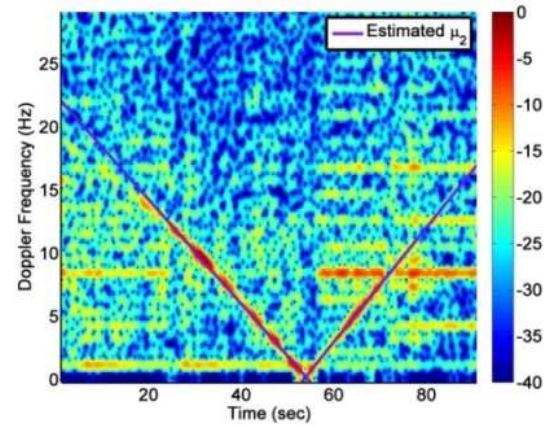


Fig. 11 - Spectrogram of the signal received from R_{x2} .

The cross-correlation in Fig. 15 is shown as function of time. For this case study we obtain a cross-correlation peak of $\rho=0.7874$ and an estimated time delay equal to $\Delta t = 0.0998$ sec. Exploiting the relation in (8), where the mean of the two estimated Doppler rates ($\bar{\mu} = 0.4333$) is used, the velocity cross-baseline and the baseline crossing point are estimated,

respectively as $\tilde{v}_x = 81.15 \text{ m/s}$ and $\tilde{y}_0 = 6.12 \text{ km}$. The velocity provided by the ADS-B is equal to $v = 79.07 \text{ m/s}$ and, in accordance with the geometry previously introduced in section 5.1, as the baseline crossing angle is 10° (i.e. the velocity cross-baseline is $v_x = 77.87 \text{ m/s}$) and the baseline crossing-point is $y_0 = 5.19 \text{ km}$, a good estimation of v_x and y_0 is achieved with 4.21% and 17.83% relative error, respectively. This shows the practical effectiveness of the technique and validate the proposed approach.

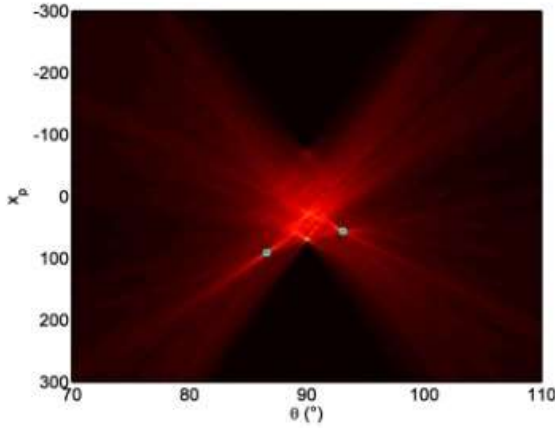


Fig. 12 - Radon transform of the spectrogram related to the signal received from Rx_1 .

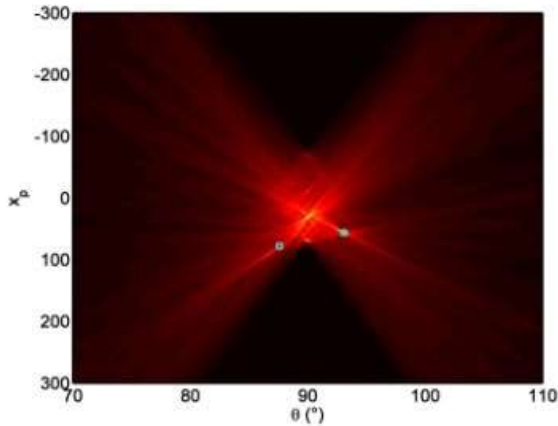


Fig. 13 - Radon transform of the spectrogram related to the signal received from Rx_2 .

6 Conclusions

In this paper the issue of motion parameters estimation was addressed in a dual-baseline FSR configuration: a new approach was presented based on the Doppler signature spectrogram and the time delay estimated from the cross-correlation between the signals acquired by the two different receivers. The effectiveness and the feasibility of the proposed approach for the estimation of the cross-baseline velocity and the baseline crossing point without a priori knowledge was shown from both synthetic data set and real data obtained from a dual-receive passive FSR configuration. Also some aspects of potential solutions from the spectrogram domain when more than two targets cross the baseline were discussed.

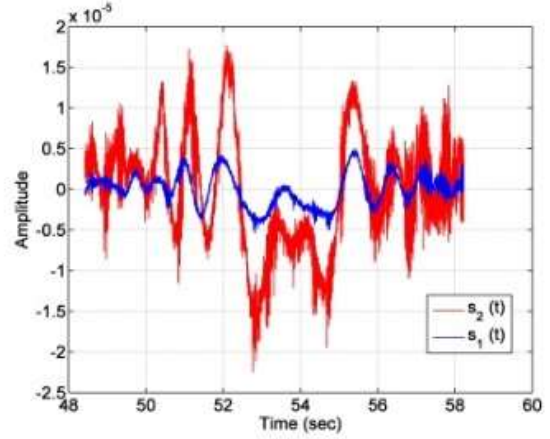


Fig. 14 - (a) Part of the signal around crossing-time.

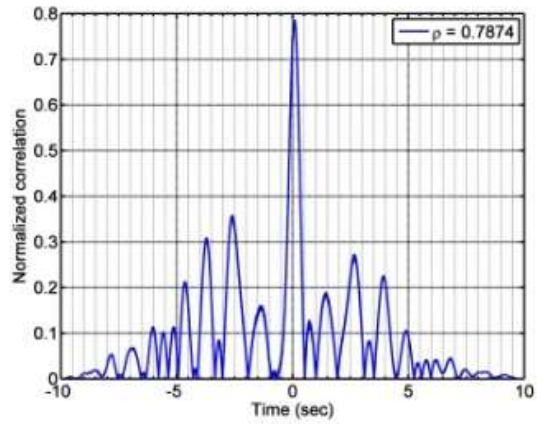


Fig. 15 - Normalized cross-correlation.

References

- [1]. M. Gashinova, L. Daniel, V. Sizov, E. Hoare and M. Cherniakov, "Phenomenology of Doppler forward scatter radar for surface targets observation," in *Radar, Sonar & Navigation*, IET, vol.7, no.4, pp.422-432, April 2013.
- [2]. M. Contu, A. De Luca, S. Hristov, L. Daniel, A. Stove, M. Gashinova, M. Cherniakov, D. Pastina, P. Lombardo, A. Baruzzi, D. Cristallini "Passive Multi-frequency Forward-Scatter Radar Measurements of Airborne Targets using Broadcasting Signals", *IEEE Transactions on Aerospace and Electronic Systems*, in print.
- [3]. D. Pastina, M. Contu, P. Lombardo, M. Gashinova, A. De Luca, L. Daniel and M. Cherniakov, "Target motion estimation via multi-node forward scatter radar system," in *IET Radar, Sonar & Navigation*, vol. 10, no. 1, pp. 3-14, 1 2016.
- [4]. A. De Luca, M. Contu, S. Hristov, L. Daniel, M. Gashinova and M. Cherniakov, "FSR velocity estimation using spectrogram," 2016 17th International Radar Symposium (IRS), Krakow, 2016, pp. 1-5.